

MM Engineering College

Team-MOLTRES 2014

(ESVC030)

Final Design Report



Abstract-

The objective of **ESVC 2014** competition is to simulate the real world engineering design projects and their related challenges. Our goal is to Design an economical vehicle with best performance. The team is focused to design the vehicle by keeping in mind the ESVC requirements, driver's comfort and safety, and to increase the performance and drivability. To achieve our goal the vehicle has been divided into subcomponents and each member is assigned a specific subcomponent (Chassis, Suspension, Wheel Assembly, Steering and Brakes, Power transmission Solar or Electrical). For designing, analysis and optimization of the vehicle components various software like Solid Works and Ansys (design and analysis), Lotus (steering and suspension design) has been used.

As a whole, the main objective of the team is to reduce the weight of the vehicle, augment the performance and minimize the power loss.

INTRODUCTION: -

ESVC event is organized by ESVC LPU. The teams are given the challenging task to design and fabricate a single seat, off-road, solar powered and fun to drive vehicle which is intended for sale to weekend off road enthusiasts.

The design process of this single-person vehicle is iterative and based on several engineering and reverse engineering processes.

1. Endurance
2. Safety and Ergonomics
3. Market availability
4. Cost of the components
5. Standardization and Serviceability
6. Maneuverability
7. Safe engineering practices.

TRACK WIDTH-

The track width of the car is an important criterion as it is the amount of resistance

offered to the overturning moment at the Center of Gravity due to the inertial force and at the tires due to lateral weight transfer. Considering these points and the design restrictions we have decided to keep a track width of 1231.9 mm

WHEELBASE-

Wheelbase is determined early during the time of design as it influences two things importantly. One, it decides the longitudinal weight transfer during braking and acceleration and Two, we get to know about the packaging of the components in our vehicle. So we have decided to keep a wheel base of 1676.4 mm

DESIGN REPORT:

MAIN FRAME:

The frame or chassis can be called as skeleton of a vehicle, beside its purpose being seating the driver, providing safety and incorporating other sub system of the vehicle. The whole frame is made from tubular pipe.

Material for main frame-

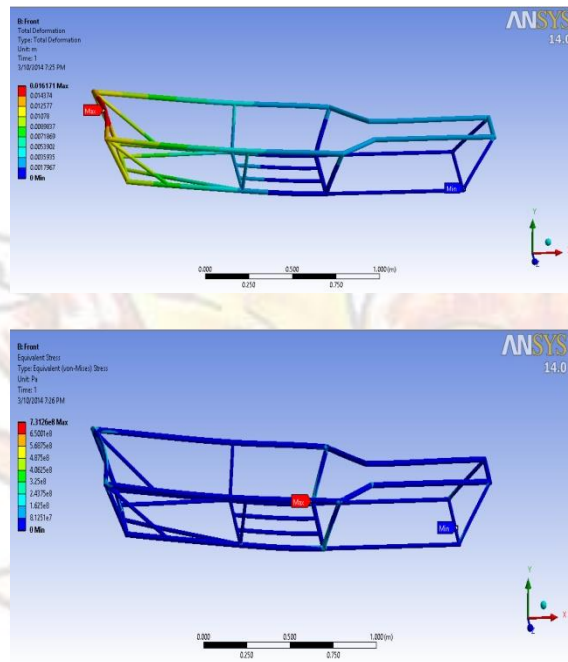
1"x0.0787", 1"x0.039" and 0.75"x0.071"
1020 DOM

MECHANICAL PROPERTIES OF 1020 DOM STEEL:

Properties	Value	T (°C)
Density ($\times 1000$ kg/m³)	7.7-8.03	25
Elastic Modulus (GPa)	190-210	25
Tensile Strength (MPa)	550	25
Yield Strength (MPa)	480	25
Elongation (%)	15in2	25
Hardness (HB)	B80	25

CHASSIS LOADING & SIMULATION:

1. FRONT IMPACT:



Calculation:

$$F = (MV_2 - MV_1)/t$$

Here, $V_2=0$; (since, it is assumed that after impact it will come to rest)

$F = (-MV_1)/t$; (here negative sign indicates that direction of impact force will be approx. to the velocity.)

Neglecting the negative sign, we have;

$$F = MV_1/t$$

The time t can be written as $t=2x/u + V$

Here $V=0$ and $u=V_1$,

Therefore, $F = MV_1/2x$; (x is distance travelled before stopping)

Now, putting values, we have;

$$M = 200 \text{ kg}, u = 42 \text{ km/hr} = 11.67 \text{ m/s}, x = 1 \text{ m}$$

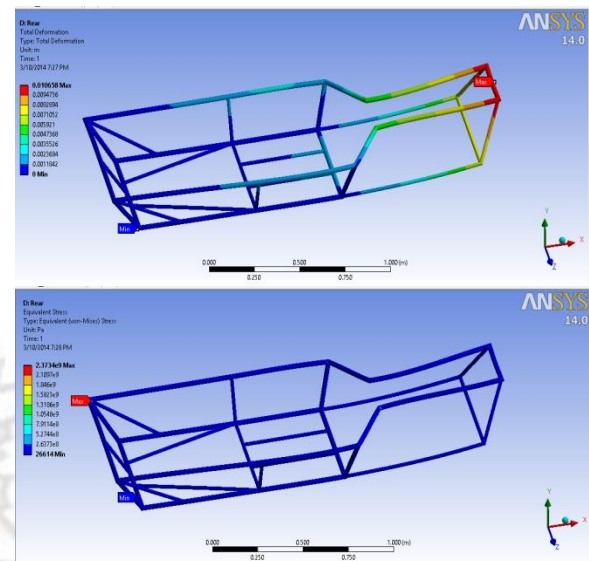
$$F = 13729 \text{ N}$$

Results:-

Maximum Deformation= 16.17mm

$$\text{FOS} = 1.7$$

2. REAR IMPACT:



Calculation:

$$\text{Force, } F = (MV_2 - MV_1)/t$$

Let us assume that after back impact velocity gets 1.5 times more, therefore

$$V_2 = 1.5V_1$$

$$F = MV_1/2t$$

Assume that vehicle moves distance x during this change, therefore time taken to cover this distance x ,

$$t = 2x/(u+v) = 2x/(2.5u) = 0.102 \text{ sec}$$

$$F = (5/8) \times (\mu^2/x)$$

Now putting values $m = 200$ Kg,

$$u = 42 \text{ km/hr} = 11.67$$

$$\text{m/s}, x = 1.5 \text{ m},$$

$$F = 11349.075 \text{ N}$$

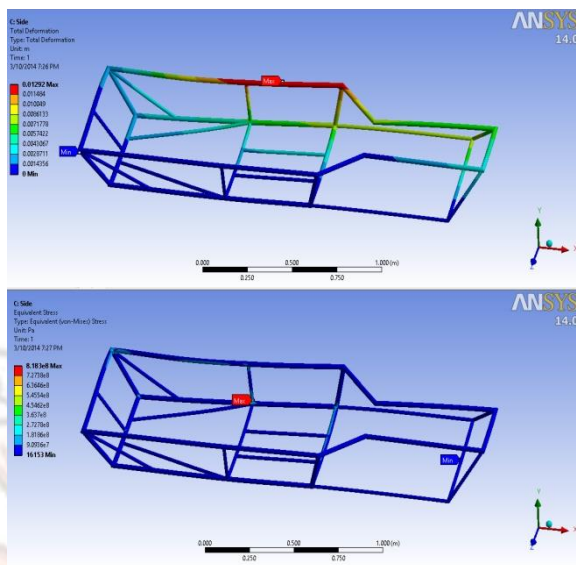
Results:-

Maximum Deformation= 10.65mm

Max. Equivalent Stress= 237.34 MPa

$$\text{FOS} = \sigma_{yt}/\sigma_{\max} = 480/237.34 = 2.02$$

3. SIDE IMPACT:

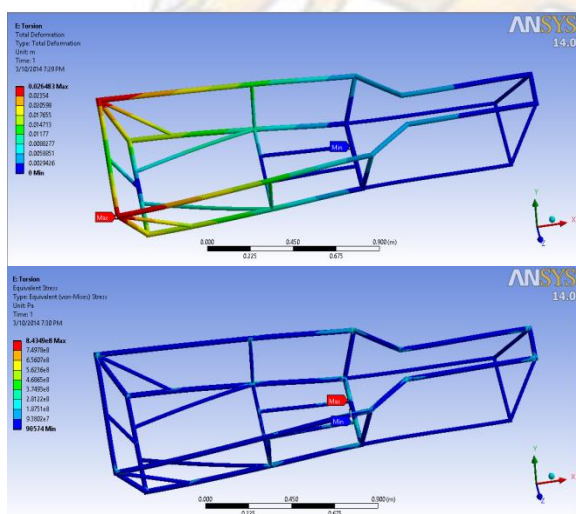


For side impact, model of vehicle is considered as a point mass (i.e. having same mass concentrated at one point). The side collision of vehicle is modeled as a perfectly inelastic one and necessary calculations have been carried out using conservation of energy and conservation of momentum principle. The test is made at a force of 5000 N.

Results:-

Maximum Deformation= 12.92mm
FOS = 1.6

4. TORSION TEST:



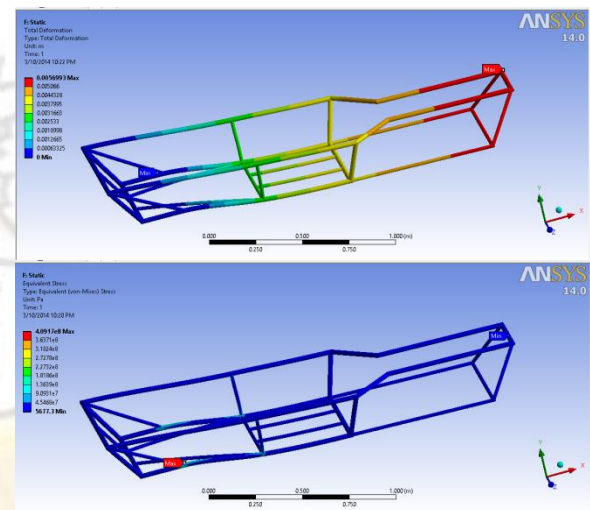
Four outer joints of back portion are

fixed and opposite forces are applied at to outer links of front portion. Force on each outer link $F=2000N$

Results:-

Maximum Deformation= 16.48mm
FOS = 1.5

5. STATIC LOADING:



Total mass assumed $\rightarrow 200kg$
Now, total vertical static force including gravitational
 $200 \times 9.81 = 1962N$

Results:-

Maximum Deformation= 5.699mm
Max. Equivalent Stress= 409.17 MPa
 $FOS = \sigma_{yt} / \sigma_{max} = 480 / 409.17 = 1.17$

OVERALL ALL RESULT:

SR.NO.	TEST	Max. Deformation	FOS
1	Front Impact	16.17	1.7
2	Rear impact	10.65	2.02
3	Side Impact	12.92	1.6
4	Torsion	16.48	1.5
5	Static Loading	5.669	1.17

ELECTRICAL REPORT

GENERAL OVERVIEW:-

Solar cars utilize sun's energy. Solar array, a combination of solar cells, collects sun's energy and converts it into usable electrical energy. This usable electrical energy is stored in batteries. Batteries connected to the motor. Motors can be run and controlled by the use of a motor controller that adjusts the amount of energy flowing to the motor according to the throttle.



Circuit Connection

SOLAR ARRAY:-

The capacity of batteries set out by race rules and regulations is too small for a solar car to fully depend on during a race. Energy must be obtained from the sun by solar array to supplement the energy taken from the batteries. Under maximum insolation levels, the solar array can sometimes supply ample energy, and the excess simply flows back into the batteries. The solar array consists of a configuration of solar photovoltaic cells, usually encapsulated to protect against the elements and damage.

The encapsulation of cells also increases the overall efficiency of the array. This is achieved by carefully designing anti-reflective coatings and materials to maximize the light energy captured. General categories of solar cells include amorphous, multi-crystalline and polycrystalline cells. Some types solar cells include screen printed, buried contact cells (BCC), laser-grooved cells and passive emitter reflective layer (PERL). A screen printed Polycrystalline cell showing the fine metal fingers and bus bars which collect the energy from the surface of the cell is shown in Figure. The cell shown has a rated efficiency of ~16.5%. Commercially manufactured cells are available with maximum efficiencies in the order of 26%, however cells have been produced with peak efficiencies of 30-35% under laboratory conditions. Solar cells convert sunlight (photons) to electricity (electrons) by the raising of the energy level of electrons in the crystalline lattice, and allowing them to move freely throughout the structure. Solar cells are constructed from a semiconductor p-n junction, which allows current to flow in one direction only, similar to the operation of a diode. The new array should have higher efficiency cells and enhance encapsulation materials. The Team used Polycrystalline panel because of its following advantages over monocrystalline.

Take solar irradiation is 1000 watts/m²
and temperature of atmosphere is 25.C.

So Power of panel is given by

$$P=V*I$$

P=power in watts

V=voltage in volts

I=current in ampere

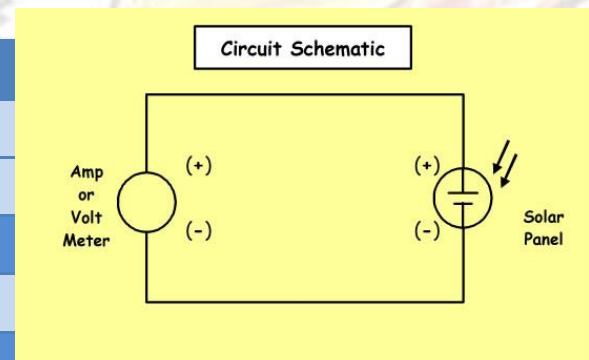
CHARACTERISTIC:

Circuit arrangement for characteristic of panel-

POLY-CRYSTALLINE	MONO-CRYSTALLINE
Low cost	High cost
Easily available in market	Not easily available
It is light in weight	It is heavier comparatively

The specification of solar panel-

SPECIFICATION	
TYPE	PP74W12V
MAX. POWER (P _m)	77.760W
MAX. VOLTAGE (V _m)	19.804V
MAX. CURRENT (I _m)	3.927A
OPEN CIRCUIT VOL. (V _{oc})	24.114V
SHORT CIRCUIT CUR. (I _{sc})	4.765A
MODULE EFFICIENCY (%)	13.62
CELL TYPE	POLYCRYSTALLINE
CELL DIMENSION(MM)	660*865
DIMENSIONS(MM)	1465X650X35
WEIGHT(Kg)	6



OBSERVATION TABLE:

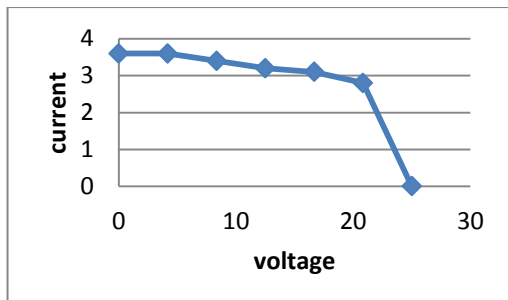
VOLTAGE	CURRENT	POWER
0	3.8	0
4.17	3.8	15.846
8.34	3.6	30.024
12.51	3.4	42.534
16.67	3.2	53.344
20.84	2.8	58.352
25.01	0	0



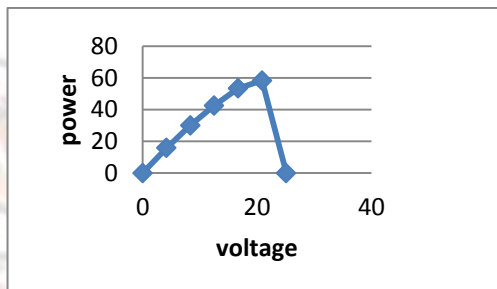
SOLAR ARRAY DIAGRAM:

CALCULATION:

GRAPH:

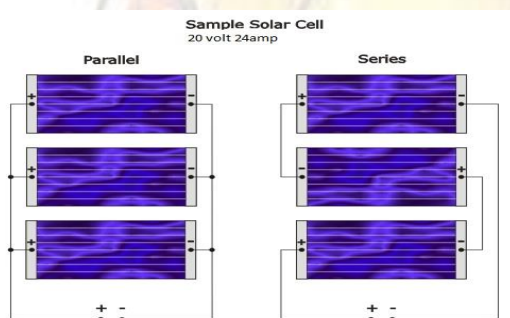


V-I CURVE



V-P CURVE

CONNECTION OF PANELS:



CHARGER:-

Charging a lead acid battery is a matter of replenishing the depleted supply of energy that the battery had lost during use. This replenishing process can be accomplished with several different charger implementations: "constant voltage charger", "constant current charger" or a "multistage" constant voltage/current charger". Each of these approaches has its advantages and disadvantages that need to be compared and weighed to see which one would be the most practical and realistic to fit with our requirements. Both constant voltage and current approaches have their

advantages; that is the reason multistage chargers have been developed which combine the two methods to achieve maximum charge time, with minimum damage to the charging cell.

Stage 1: Deep Discharge Charging Pulse Mode

The Charger starts charging at 0.5V and give pulse current up to 5V. This has effect of removing loose sulphation formed during deep discharge state of the battery.

Stage 2: Constant Current Mode (CC)

The charger changes to constant current 2.5A. When the battery voltage reaches up to 14.4V, the charging stage changes from (CC) Constant Current to CV (Constant Voltage) mode.

Stage 3: Constant Voltage Mode (CV)

The charger holds the battery at 14.4V and the current slowly reduces. When the current reaches at 0.5 C (C= Battery Capacity), this point called the Switching Point. The Switching Point is one of the great features of this battery charger that it can adjust the current automatically according to the battery capacity. Other chargers without microprocessors are not capable to adjust the current.

Stage 4: Standby Voltage Mode

The charger maintains the battery voltage at 13.8V and current slowly reduces to zero. Charger can be left connected indefinitely without harming the battery.

Recharging:

If the battery voltage drops to 13.8V, the charger changes from any mode to Constant Current mode and restart charging. The charging cycle will go through Stage 2 to Stage 4.

As much as multi-stage chargers are enticing in terms of their features, for our

purposes, the complexity and the control logic needed to implement this kind of solution would make our project unrealistic given the time constraints.

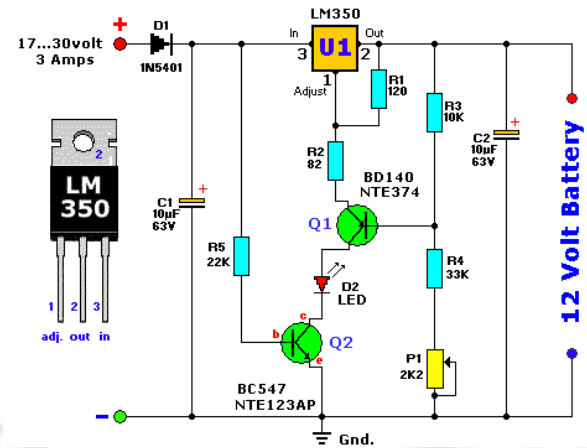
so moltres team used voltage regulator which is LM350.

VOLTAGE REGULATOR:

The LM350 is an adjustable three-terminal positive voltage regulator capable of supplying in excess of 3.0 A over an output voltage range of 1.2 V to 33 V. This voltage regulator is exceptionally easy to use and requires only two external resistors to set the output voltage. Further, it employs internal current limiting, thermal shutdown and safe area compensation, making it essentially blow-out proof. The LM350 serves a wide variety of applications including local, on card regulation. This device also makes an especially simple adjustable switching regulator, a programmable output regulator, or by connecting a fixed resistor between the adjustment and output, the LM350 can be used as a precision current regulator.

Features:

- Guaranteed 3.0 A Output Current
- Output adjustable between 1.2V and 33V
- Load Regulation Typically 0.1%
- Line Regulation Typically 0.005%/
- Internal Thermal Overload Protection
- Internal Short Circuit Current Limiting Constant with Temperature
- Output Transistor Safe Area Compensation Floating Operation for High Voltage Applications
- Standard 3-lead Transistor Package
- Eliminates Stocking Many Fixed Voltages.
- **Pb-Free Packages are Available**



BATTERY:-

The primary energy source for the vehicle is the battery bank. The battery bank usually consists of a number of individual batteries connected in series or parallel. Each battery in the bank is typically 6 or 12V, and multiple batteries are connected in series or parallel to obtain the desired system voltage. A single battery is actually made from multiple “cells” contained within the battery housing. A sealed lead acid type showing Photovoltaic Solar Array Maximum Peak Power Trackers (MPPT's) Battery Bank (48V DC)

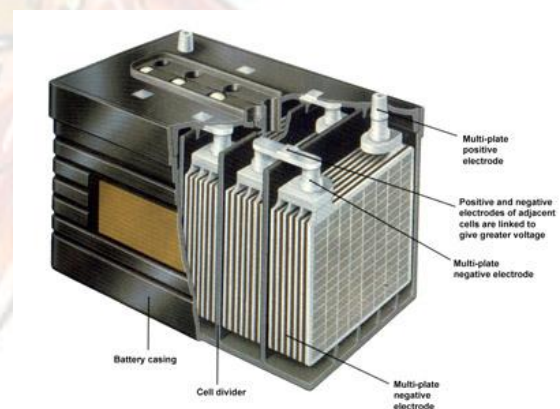


Figure : A Sealed Lead Acid Battery

The internal structure is shown in Figure. The overall battery voltage is chosen

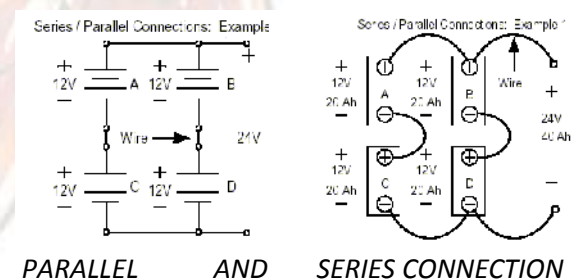
depending on the motor's EMF constant and the desired nominal cruising speed. For the most efficient operation of the drive system, the battery voltage is chosen so that the motor controller can operate with minimal PWM (i.e. reduced switching losses), at the maximum desirable speed of the car. In practice however, the battery voltage, especially for lead-acid batteries, fluctuates considerably around the nominal battery voltage, from full charge to maximum discharge. For this reason, the nominal battery voltage is usually chosen so that the lowest possible battery voltage is able to sustain a reasonably competitive speed. An alternative solution to this problem is to implement a boost/buck converter in the motor controller so that an optimal speed can be obtained for any battery voltage. There are many types of commercial batteries available today. Some examples particularly applicable for solar racing vehicles are sealed (maintenance free) lead-acid, silver-zinc, lithium-iron and zinc-air. The MOLTRES team's solar car, chose to obtain sealed lead-acid batteries due to easy of availability and relatively cheap cost. One major drawback however is a relatively large weight/energy density ratio, and a full set of batteries typically weighed in at 27.6kg. Each type of battery has different characteristics (e.g. energy density/kg, charge/discharge rate) and uses, however a comprehensive study of batteries is beyond the scope of this thesis.



Specification of battery that we used is given below:

SPECIFICATION	
BATTERY TYPE	LEAD- ACID
RATED VOLTAGE	12V
CAPACITY	24AH
CHARGING CURRENT	7A
DISCHARGING CURRENT	30A

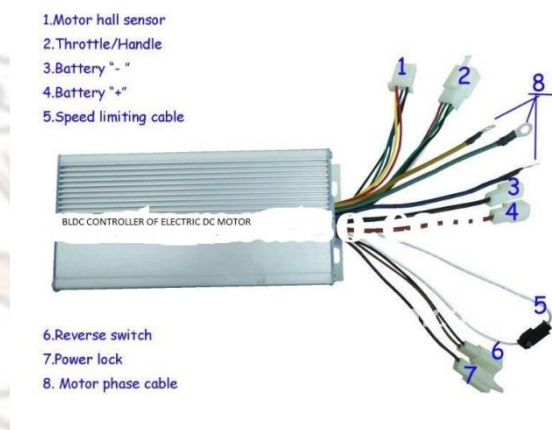
CONNECTION OF BATTERY:



MOTOR CONTROLLER:

The motor controller is designed to convert the electrical energy obtained from the batteries and solar array to

suitable power waveforms to drive the motor. The motor controller used in the solar car is designed to drive a Permanent Magnet Brushless DC (PM-BLDC) motor. The driver becomes part of the speed regulation loop as the torque produced in the motor can be controlled via controls in the cockpit at the driver paddle.



The nominal input voltage to the motor controller was 55VDC. A PWM chip (NE5568) was used together with a ROM (N82S123AN) programmed with a commutation truth table to decode the Hall Effect signals from the motor, and provide excitation to the correct phases. All logic circuitry was supplied power using a linear 5V regulator, which has an efficiency of ~50%. The inverter stage was a common three phase H bridge design, using three paralleled MOSFET's (IRFP260) in one switch, i.e. a total of 15 MOSFET's. The MOSFET's had transient suppressing metal oxide varistors (MOV) to clamp the voltage over each MOSFET switch to a safe level. DC link capacitors (12 X 220uF

Standard electrolytic) were used in the DC link. The MOSFET gates were driven by an IR2130 3-phase bridge driver chip. All three lower inverter switches had a 20k

ohm resistor connected in parallel, which meant each time the upper switches were activated, 0.72 W power dissipation occurred. A simple shunt resistor was used to measure the constant current in the DC bus, instead of in the DC link. Driver controls consisted of two potentiometers: one to adjust speed and the other to adjust the current limit value.

A direction switch was also available however care had to be exercised when moving at fast speeds to not bump the switch in the opposite direction, otherwise excess currents would flow and destroy the controller.

Throughout the thesis document, the following numbering pattern for MOSFET's in the H-Bridge will be as follows:

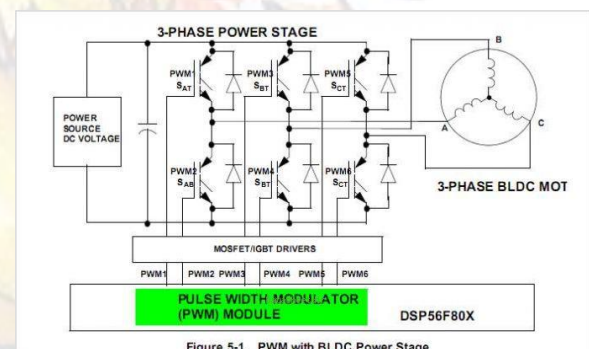


Figure: Numbering pattern for MOSFET's in the H-Bridge

Each of the MOSFET's contain an intrinsic diode which has a reverse recovery time comparable to that of a discrete diode placed in parallel with the MOSFET. The diodes will be referenced with the same numbering as the MOSFET's, i.e. SW1 has a corresponding diode D1, and so on. The specification of controller is

SPECIFICATION	
Controller type	PWM
Rated voltage	55V
Rated current	12A
Rated power	650W

THROTTLE:

A throttle is the mechanism by which the flow of a fluid is managed by constriction or obstruction.

An **engine's** power can be increased or decreased by the restriction of inlet gases (i.e., by the use of a throttle), but usually decreased. The term throttle has come to refer, informally and incorrectly, to any mechanism by which the power or speed of an engine is regulated. What is often termed a throttle (in an aviation context) is more correctly called a **thrust lever**. For a **steam engine**, the steam valve that sets the engine speed/power is often known as a regulator.



MOTOR:

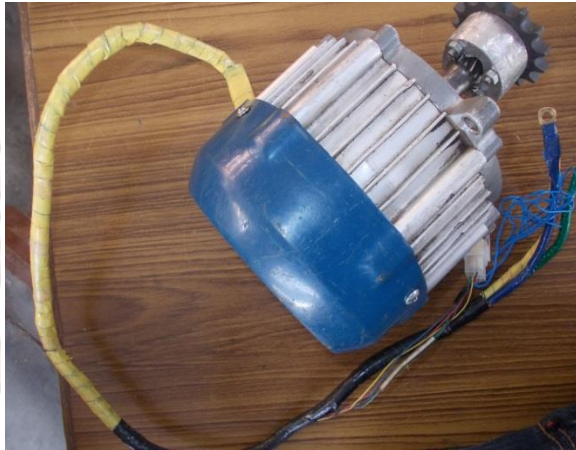
The motors' function is twofold: to convert the electrical energy to mechanical energy when motoring and mechanical energy to electrical energy when regenerating. There are a number of types of motors in use today, ranging from the induction, switched reluctance, brushed DC and stepper motors. Each

motor has a number of advantages and disadvantages in particular applications ranging from large industrial roller mills to accurate positioning control. The most popular choice for high efficiency applications such as solar cars is the permanent magnet brushless DC motor or sometimes known as a synchronous DC motor. The advantages of the BLDC motor include:

- Very high efficiency characteristics over a large power range (98.2% recorded for an optimized Halbach magnet arrangement).
- Require minimal maintenance, due to elimination of mechanical commutator and brushes.
- Long operating life and higher reliability.
- No brushes mean no arcing which can be paramount when working in flammable gas locations.
- Number of motor geometry's possible (e.g. interior permanent magnet or surface magnet arrangements).
- High power density and torque to inertia ratio give a fast dynamic response.
- No brushes eliminate need for a high rotor inertia.
- Speed restrictions due to the traditional mechanical commutator are eliminated.

BLDC MOTOR

There are a number of configurations for the brushless DC motor, however all operate on the same principal. There are three main components that make up such a motor.



Stator Winding: The stator is usually wound in a three phase wye (or star) connection. Three phase windings are usually sufficient to control most motors, however more than three phase windings are common, and simply require additional H-bridges and commutation circuitry. There are each phase is broken up into multiple sections. There is also the option to connect the windings in a delta configuration; however this may introduce unwanted circulating currents flowing around the windings. The stator of the CSIRO motor is shown in Figure. Each of the three phase windings are distributed in a



STATOR WINDING DIAGRAM

Sinusoidal pattern around the circumference of the stator are encapsulated in a fiberglass resin. By winding the phases in a sinusoidal pattern, a sinusoidal back emf voltage waveform is produced between two phases when the motor is turned by hand. To obtain maximum efficiency, sinusoidal phase current excitation must be applied to the motor.

Rotor Magnets: In conventional DC motors, electromagnets are used to create a magnetic field. The rotor in a BLDC motor consists of rare earth magnets which produce a constant flux (hence the name permanent magnet). One of the rotor magnet rings of the CSIRO motor is shown in Figure (r). The NdFeB magnets (neodymium-iron-boron) are glued to the backing iron, and are arranged in a circle comprising 40 magnet pieces (i.e. 40 pole motor), in an alternating N – S – N configuration. The backing iron forms part of the magnetic circuit. There are two identical magnet rings which are placed on either side of the stator and are kept separated by special rims. The stator will be held stationary and fixed to the trailing

arm.



ROTAR MAGNET DIAGRAM

Both rotor magnet rings are fixed to the wheel rim, and rotate with the movement of the tyre.

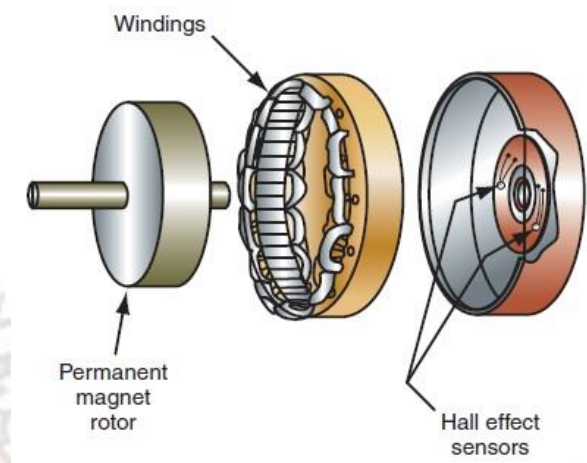
HALL EFFECT SENSORS:

Hall sensors are a popular choice for rotor position feedback in brushless DC drives, reasons being they are cheap and do not require complex processing algorithms. Hall sensors are more suited for use with trapezoidally controlled motors, as sinusoidal machines usually require a higher resolution sensor such as a shaft encoder or transducer. The actual sensor is usually an N-doped InSb semiconductor, which in the presence of a magnetic flux, an electromotive force causes free flowing electrons to move to one side of the semiconductor which causes a potential to form on the output terminals.

In most hall elements manufactured, a voltage regulator, amplifier and schmitt trigger are all integrated inside the one device. The Hall Effect sensors are glued to a PCB which is located inside the motor. The PCB can be adjusted manually to align the stator coil position with the Hall Effect position. The PCB with the hall

effect sensors mounted is shown in fig1

(a)



Hall Effect sensor diagram 1(a)

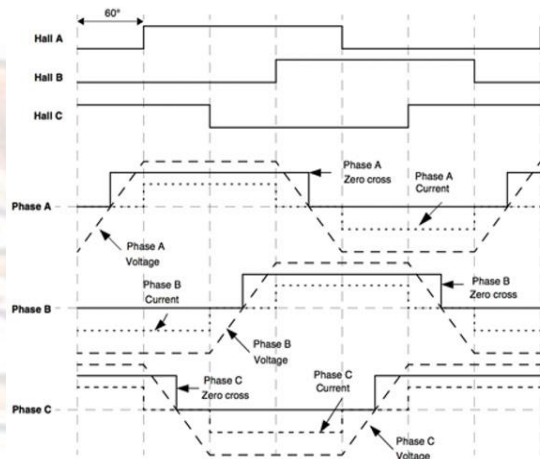
Three Hall effects give output six different states for one full electrical cycle, which is usually sufficient for most motor control applications. There are two possible ways of positioning the Hall Effect sensors around the axis. The hall elements can either be placed at 60 or 120 electrical degree intervals (i.e. the hall code changes every 60 or 120 electrical degrees). The Hall effects to be used are configured to change every 60 electrical degrees. One electrical cycle is equal to 360 electrical degrees, and is defined as when the hall sequence starts to repeat. The Hall Effect sequence can be represented in Figure 1(b). Since the motor has 40 poles, for one revolution of the motor, each hall sensor will experience 20 North's and 20 South's (i.e. 20 high and 20 low level outputs).

The mechanical separation of the magnets and Hall Effect sensors can be calculated easily from knowing the number of magnets and poles. One mechanical cycle

is equal to one entire revolution of the motor or 360 mechanical degrees. One electrical cycle repeats every every

$$\frac{\text{no of electrical in one cycle}}{\text{pole}} \times 2 = \frac{360}{20}$$

=18 mechanical degrees.



SPECIFICATION

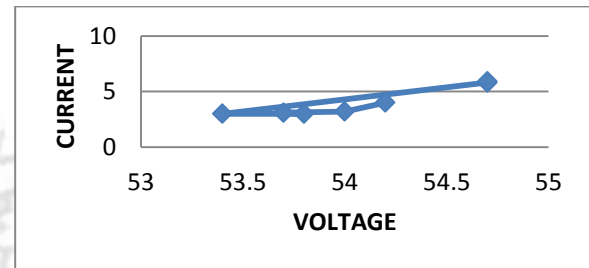
Operating voltage	48V
Rated current	10A
Max. speed	3500 rpm
Max. torque	5 N-M
Max.power	500W

CHARACTERSTICS OF MOTOR:

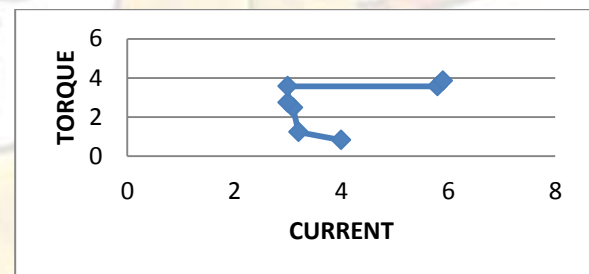
VOLTAGE	CURRENT	TORQUE	RPM
54.2	4	0.825	1550
54	3.2	1.2375	1000
53.7	3.1	2.475	500
53.8	3	2.75	156

53.4	3	3.575	52
54.7	5.8	3.575	150
54.7	5.9	3.85	100

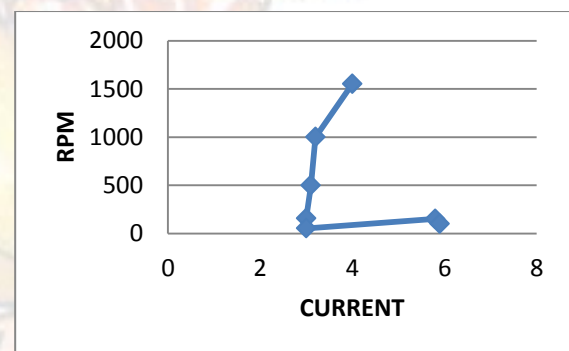
GRAPH:



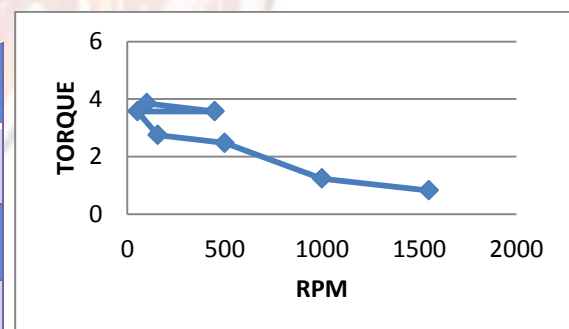
CURRENT-VOLTAGE CURVE



TORQUE-CURRENT CURVE



CURRENT- RPM CURVE



TORQUE-RPM CURVE

BRAKING:

OBJECTIVE: The brakes are one of the most important safety systems on the vehicle. Our vehicle uses three disc brakes, to bring the vehicle to a quick and safe stop regardless of weather conditions or topography.

The vehicle has two independent hydraulic systems and it is actuated by a single brake pedal. The pedal directly actuates the master cylinder. Here no cables are used for this purpose. All rigid brake pipes are mounted securely along the roll cage or along other members.

SELECTION OF DISC BRAKES OVER DRUM BRAKES:

- In case of disc brakes friction surfaces are directly exposed to the cooling air whereas in the drum type, the friction occurs on the internal surface, from which heat can be dissipated only after it has passed by conduction through the drum.
- The friction pads in case of disc brakes are flat as compared to curved friction linings in case of drum brakes. This means that in disc brakes, there is a uniform wear of friction pad. Moreover, the friction pad material is not subjected to any bending, thereby increasing the range of material from which a suitable one can be chosen. Generally, we use asbestos fibre with metal **oxide filler bonded with organic compounds** as the material for friction pads.
- Unlike the conventional drum brake, the design of disc brake is such that there is no loss of efficiency due to expansion. As the system becomes hot, the drum

expands internally and the expanding shoe type of brake tends to move the friction surface apart, causing a loss of effective pedal travel. On the other hand, disc expansion merely changes the relative position on the friction surfaces slightly without tending to increase the clearance.

- Disc brakes weigh less than their conventional drum type.
- Disc brakes have comparatively better anti-fade characteristics.
- Compared to drum type, the disc brakes are simple in design. There are very small numbers of parts which can wear or not function properly.
- It is very easy to replace the friction pads when required, compared to the drum type where the brake linings have to be either riveted or fixed with adhesive to the brake shoes.
- Total frictional area of pads in disc brakes is very less as compared with the conventional drum type brakes, the approximate ratio being 1:4. This means that in disc brakes, the pressure intensity must be considerably greater than in the drum type. This implies that frequent relining would be necessary, due to increased rate of wear.
- However, there are compensating factors:
Pads can be made considerably thicker, for a given initial cost, so that more wear can take place before replacement is necessary.
New wear-resistant friction materials have been developed, that are more

suitable for disc brakes than drum brakes.

MARKET SURVEY:

Discs, Callipers and Master Cylinders which were considered suitable for the vehicle after exhaustive market surveys are as stated below:

5	Apache RTR 180	220	10
6	Honda Aviator	190	10
7	Firefox TREK	170	8

ROTORS:

The discs of brakes are made of paralytic gray cast iron. The material is cheap and has good anti-wear properties. Cast steel discs have also been employed in some cases, which wear still less and provide higher coefficient of friction; yet the big drawback in their case is the less uniform frictional behaviour. Two types of discs have been employed in various makes of disc brakes, i.e. the solid or the ventilated type.

Disadvantages of ventilated type discs:

- Usually thicker and even sometimes heavier than solid discs.
- In case of severe braking conditions, they are liable to warp.
- Dirt accumulates in the vents, which affects cooling, resulting in wheel imbalance.
- Expensive.
- Difficult to turn. Turning produces vibrations which reduces the life of the disc.

We selected Disc of Honda Aviator for the following reasons:

- Thickness (10mm) of the disc is not too high. So disc can be turned safely.
- An Outer diameter is 190mm which is in accordance with our required design.
- The disc can be safely turned to 190mm which is as per our design.



Sr. No.	Disc	Out dia (in mm)	Thickness (in mm)
1	Maruti 800	220	15
2	Mahindra	250	20
3	Pulsar 220	230	8
4	Pulsar 150	240	10

CALIPER:

We have used a **fixed type calliper** in our design. Fixed type calliper doesn't move but has piston(s) arranged on opposing sides of the rotor. Fixed callipers are preferred for their performance, but are more expensive than floating one.

Sr. No	Calliper	No. of piston	Arrange-ment of pistons	Dia. of piston front
1	Pulsar front	2	Single side	21
2	Apache RTR 180	2	Single side	29
3	Maruti 800	1	Single side	60
4	Pulsar rear	1	Single side	40
5	Honda Aviator	3	Single side	28
6	Honda Aviator	2	Single side	28

Reasons for finalizing Honda Aviator calliper:

1. It is small enough so properly fits in the wheel assembly.
2. In accordance with the rule it has bleeding valve on the top.
3. It is having CBS (Combined Braking System). This technology is introduced by Honda and CBS is 1.7 times effective than conventional brakes.



BRAKE CIRCUITS:

□□ Cross linked hydraulic split was not considered because in case of a failure one front wheel and one rear wheel would lock

at the same time increasing the chances of skidding towards the left or the right.

□□ Diagonal split hydraulic systems are commonly used on front wheel drive vehicles, but our vehicle is rear wheel driven.

□□ Advantage of the front-rear split design is that in the event of a failed hydraulic circuit, there are still two brakes on the same axle that provide equal braking forces. For this reason, the vehicle won't turn or pull in either direction under failed-circuit braking.

□□ By the splitting of the connections as the connection is for the 3 tyres in our case so the braking is as the connection is that 1 valve for the rear Wheel and the two ports for the front tyres and one valve of tandem master cylinder will be closed.

BRAKE FLUIDS:

We have decided to use **DOT 4** brake fluid.

□□ It is inexpensive, and available at most gas stations, department stores, and any auto parts store.

□□ It is completely compatible with DOT 3 and DOT 5.1.

CALCULATIONS:

1. The Conservation of Energy

The braking system exists to convert the energy of a vehicle in motion into thermal energy, more commonly referred to as heat. From basic physics, the kinetic energy of a body in motion is defined as:

$$K.E. = \frac{mv^2}{2}$$

• Where m = the mass (commonly thought of as weight) of the vehicle in motion

• Where v = the velocity (commonly known as speed) of the vehicle in motion

Here, v = 43 km/hr. or 12 m/sec, m = 200 kg

So K.E = 14400

2. The brake pedal:

The brake pedal exists to multiply the force exerted by the driver's foot. From Elementary statics, the force increase will be equal to the driver's applied force multiplied By the lever ratio of the brake pedal assembly:

$$F_{bp} = F_d \times \{L_1 \div L_2\}$$

Where,

- F_{bp} = the force output of the brake pedal assembly
- F_d = the force applied to the pedal pad by the driver
- L_1 = the distance from the brake pedal arm pivot to the output rod clevis Attachment

- L_2 = the distance from the brake pedal arm pivot to the brake pedal pad.

$$F_d = 35\text{N}, L_1 = 7, L_2 = 1$$

$$\text{So, } F_{bp} = 35(7 \div 1) = 245\text{N}$$

3. The master cylinder:

Assuming incompressible liquids and infinitely rigid hydraulic vessels, the pressure generated by the master cylinder will be equal to:

$$P_{mc} = \frac{F_{bp}}{A_{mc}}$$

Where,

- P_{mc} = the hydraulic pressure generated by the master cylinder
- A_{mc} = the effective area of the master cylinder hydraulic piston.

$$A_{mc} = (\pi \div 4) d_{mc}^2,$$

$$\text{Since } d_{mc} = 19\text{mm}$$

$$\text{So, } A_{mc} = 283.53\text{mm}^2$$

$$P_{mc} = 0.846\text{N/mm}^2$$

4. Brake fluid, brake pipes and hoses:

Assuming no losses along the length of the brake lines, the pressure transmitted to the callipers will be equal to:

$$P_{cal} = P_{mc}$$

Where,

P_{cal} = the hydraulic pressure transmitted to the calliper.

$$P_{cal} = P_{mc} = 0.846\text{N/mm}^2$$

5. The Calliper, Part I:

The one-sided linear mechanical force generated by the calliper will be equal to:

$$F_{cal} = P_{cal} \times A_{cal}$$

Where,

F_{cal} = the one-sided linear mechanical force generated by the calliper

A_{cal} = the effective area of the calliper hydraulic piston(s) found on one half of the calliper body.

$$F_{cal} = 0.846 \times 706.5 = 610.72\text{ N}$$

6. The Calliper, Part II:

The clamping force will be equal to, in theory, twice the linear mechanical force as follows:

$$F_{clamp} = F_{cal} \times 2$$

Where,

F_{clamp} = the clamp force generated by the calliper.

$$F_{clamp} = 610.72 \times 2 = 1221.45\text{N}$$

7. The brake Pads:

The clamping force causes friction which acts normal to this force and tangential to the plane of the rotor. The friction force is given by:

$$F_{friction} = F_{clamp} \times \mu_{bp}$$

Where,

$F_{friction}$ = the frictional force generated by the brake pads opposing the rotation of the rotor.

μ_{bp} = the coefficient of friction between the brake pad and the rotor.

$$F_{friction} = 1221.45 \times 0.7 = 855\text{N}$$

8. The Rotor:

This torque is related to the brake pad frictional force as follows:

$$T_r = F_{\text{friction}} \times R_{\text{eff}}$$

Where,

T_r = the torque generated by the rotor

R_{eff} = the effective radius (effective moment arm) of the rotor (measured from the rotor centre of rotation to the centre of pressure of the calliper pistons)

$$T_r = 855 \times 100 = 85500 \text{ Nmm}$$

The torque will be constant throughout the entire rotating assembly as follows:

$$T_t = T_w = T_r$$

Where,

T_t = the torque found in the tire

T_w = the torque found in the wheel.

$$T_t = T_w = T_r = 85500 \text{ Nmm}$$

9. The Tire:

Assuming that there is adequate traction (friction) between the tire and the road to accommodate the driver's braking request, the tire will develop slip in order to react the torque found in the rotating assembly. The amount of slip generated will be a function of the tire's output characteristics (the $\mu-x$ = slip relationship), but the force reacted at the ground will be equal to:

$$F_{\text{tire}} = \frac{T_t}{R_t}$$

Where,

F_{tire} = the force reacted between the tire and the ground (assuming friction Exists to support the force)

R_t = the effective rolling radius (moment arm) of the loaded tire.

$$F_{\text{tire}} = \frac{85500 \times 2}{406.4} = 420.7 \text{ N}$$

The total braking force generated is defined as the sum of the frictional forces at the four tires which is given as follows:

$$F_{\text{total}} = \sum F_{\text{tire}} \text{ LF, RF, LR, RR}$$

Where,

F_{total} = the total braking force reacted between the vehicle and the ground (Assuming adequate traction exists).

$$F_{\text{total}} = 420.4 \times 3 = 1261.2 \text{ N}$$

Because we have only one tyre in rear

10. Deceleration of a vehicle in motion:

The deceleration of the vehicle will be equal to:

$$a_v = \frac{F_{\text{total}}}{mv}$$

Where,

a_v = the deceleration of the vehicle

$$a_v = 1261.2 / 200 = 6.32 \text{ m/sec}$$

11. Kinematics relationships of vehicles experiencing deceleration:

For a vehicle experiencing a linear deceleration, the theoretical stopping distance of a vehicle in motion can be calculated as follows:

$$SD_v = (V_v)^2 / a_v \times 2$$

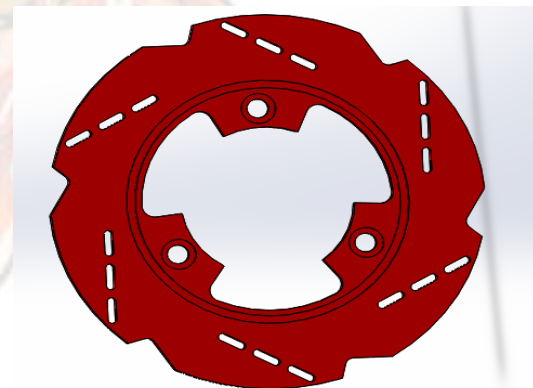
Where,

• SD_v = the stopping distance of the vehicle.

$$V_v = 12 \text{ m/sec}, a_v = 6.32 \text{ m/sec}^2$$

$$SD_v = 144 / (6.32 \times 2) = 4.4 \text{ m}$$

12. Factor of Safety:



Factor of safety = 4.3

SUSPENSION

OVERVIEW:

Suspension system must satisfy the following design requirements:

- Control movement at the wheels during vertical suspension travel and steering, both of which influence handling and stability.
- Limit chassis roll during cornering to prevent roll-over, decrease roll camber, and therefore, decrease steering reaction time.
- Prevent excessively high jacking forces by managing static roll center location and roll center migration.
- Limit lateral tire scrub to maintain straight line stability and minimize horsepower losses.
- The suspension must provide enough wheel travel to dampen the impacts imposed on the vehicle.

The non-professional weekend off road enthusiast requires a vehicle which exhibits both safe, stable, responsive handling; and a soft, comfortable ride.

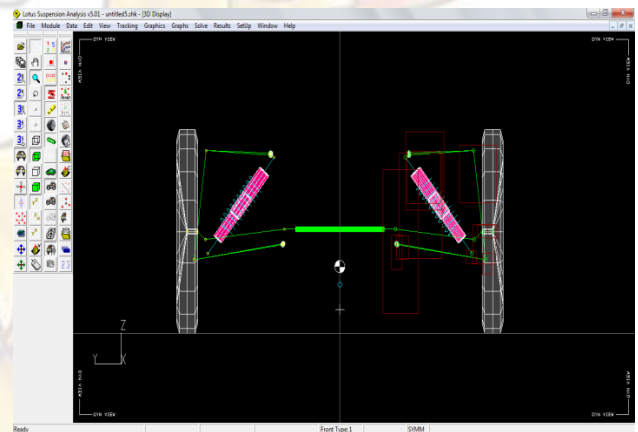
Hence the design was chosen as independent short long control arm arrangement. The suspension was designed **using lotus suspension analysis, SusProg3D & Solid Works.**

FRONT SUSPENSION DESIGN:-

Suspension in solar cars is not designed to provide a smooth ride. Soft suspensions waste energy by absorbing the motion of the car as it travels over a bump. Therefore, solar cars have a very stiff suspension, which is designed to prevent damage to the frame in the event of a large jolt. For the front wheels almost all solar cars use double A-arm suspension, shown below. The double A-arm system has normally completely independent suspension in the front or rear and are commonly used in sports and racing cars. It is a more compact

system that lowers the vehicle hood resulting in greater visibility and better aerodynamics.

In our design we are using a **Short-Long Double A-arm suspension**. The upper arm is shorter to induce negative camber as the suspension rises. When the vehicle is in a turn, body roll results in positive camber gain on the outside wheel. The outside wheel also rises and gains negative camber due to the shorter upper arm. The picture below shows the short-long arm set up for the suspension in our solar car. Solar car design uses **long uprights** mating onto high mounted wishbones reduces the thickness of the wheel fairings which lowers drag.

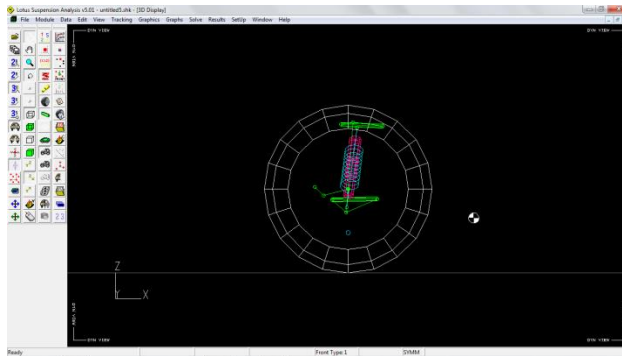


SUSPENSION GEOMETRY TERMS

The main challenge in designing a suspension system is optimizing the geometry. To understand this there are a few key terms to consider:

Caster

Positive caster induces a self-correcting force that provides straight line stability, but increases steering effort. For our design we have chosen to use a caster that is approximately **5 degrees**. This means the ball joint in the upper control arm will be positioned about an inch behind the ball joint in the lower control arm. See lotus suspension analysis drawings of the completed Suspension Assembly for more details.

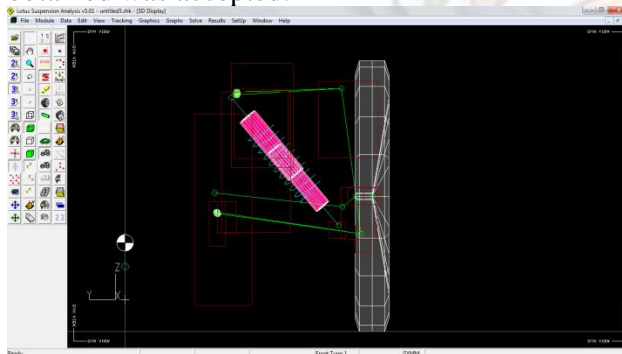


Camber

Negative camber will produce a better contact patch shape, producing additional lateral force without a large increase in slip angle and tire heating. A small amount of negative camber is desired such that on corners the outside wheel does not go into an excessive negative camber angle. **In most solar cars and in our design, the camber is 0 degrees to maximize efficiency. One main challenge of designing the suspension system is to keep the camber at 0 degrees as the wheel moves up and down over bumps.**

Kingpin Axis Inclination

A right **kingpin** inclination will reduce the steering effort and will provide the driver with a good “road feel”. Raising the KPI too much will increase the lateral forces on the cars increase making it more receptive to roll and instability. **Based on these variables, the kingpin axis inclination is roughly 7 degrees for our design** and the scrub radius so obtained was accepted.



Shocks



Intron 4402 used to test the spring stiffness

In order to determine the correct spring rate for the shocks, availability and constraining parameters were considered. The weight of the vehicle and driver was estimated to be 180 kg. The weight distribution for the car was estimated to be approximately 60/40 from the front to the rear. Using the total weight of the car and the weight distribution, the weight on each of the front tires was determined to be 50 kg. The spring stiffness of front shockers spring is 60-65 N/mm (calculated using UTM instron 4482. The desired static ride height is 6 in. This allows for a wheel travel of at least 3” for the front tires. For the required travel the total length of the shocks was set to 12” (between mountings). Our pre-load distance for the shock, which will define the spring rate based on the corner weight for the wheels, should be between 0.25in to 0.5in.

Leverage Ratio

This relates how much the wheel travels to how much the frame will move. **The leverage ratio for our design is 1.5.** Since the shocks were not satisfying our design, so we send them back to the dealer to calibrate it to fit the specific needs of our design. Based on the our contingent research and using a corner weight of 50 kg we have been able to set the following parameters listed below:

Spring Rate - 350 (lb/in)

Damping Ratio - .07 (lb*s/in)

Pre-Load - .42 in

Shock Mounting Angle - 45 degrees

Leverage Ratio - 1.5

FEA TESTS:-

These attachment joints still need to be designed and must be tested using FEA. Also we need to determine the best way to mount these to the frame.

LOWER A-ARM:

SLA wishbones were used to design the 2010 vehicle. 1"OD and 14 gauge MS 1018 pipes were used for the UCA whereas 1"OD and 12 gauge pipes were used to design the LCA of the suspension. FEA of the a-arm resulted in a FOS of 6 for the design. Gusset plates are used to reduce bending stress and increase torsional rigidity.

Threaded ball joints were used at the uprights to facilitate static camber adjustment and increase strength.

Also, **Greater the effective distance between transverse links, smaller will be the forces in the suspension control arms and their mountings.** Hence, it has been set to the value of 7.5". But the distance is restricted because of the constraints provided by the increasing in scrub radius.

UPRIGHT:

The front uprights were redesigned to incorporate the changes in suspension geometry namely kingpin and caster angle. The new upright, made of 6061 Al alloy has improved strength, serviceability; factor of safety being above 2.5 in all cases.

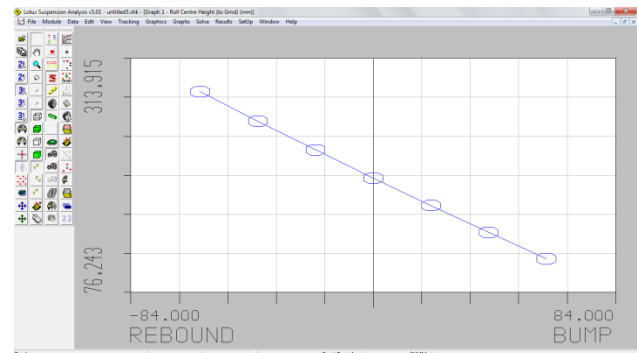
HUB:

The front hub was redesigned to meet the demands a more compact wheel assembly. It is also made of 6061 Al alloy. The strength was not sacrificed since the analysis showed FOS of 3.

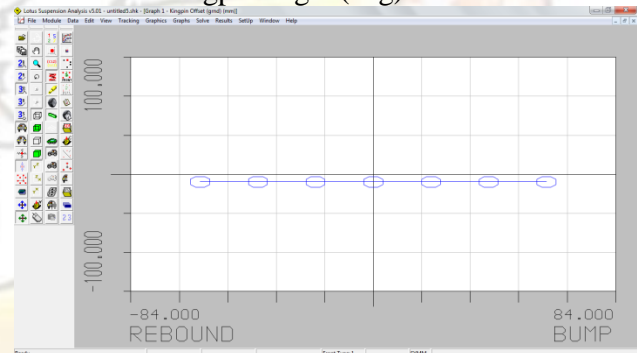
SUSPENSION ANALYSIS:-

Plot of **bump graph** for various suspension geometries

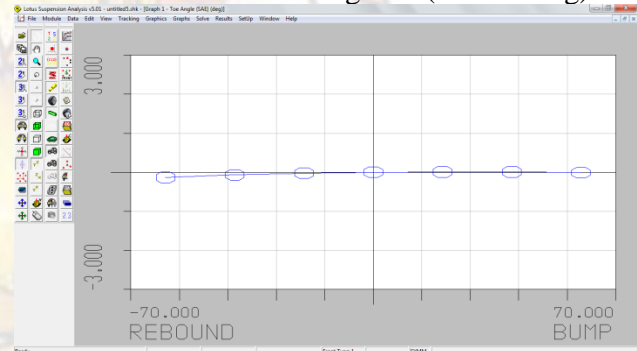
GRAPH 1: Roll center height



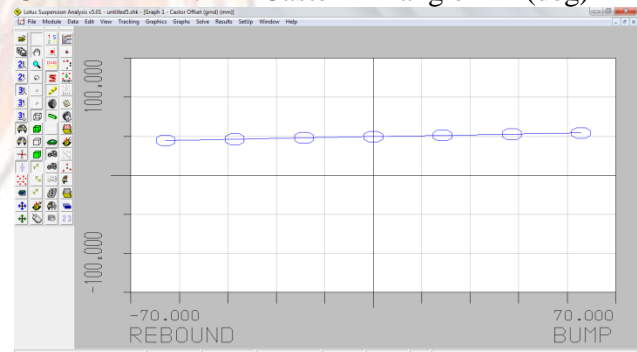
GRAPH 2: Kingpin angle (deg)



GRAPH 3: Toe angle (SAE deg)

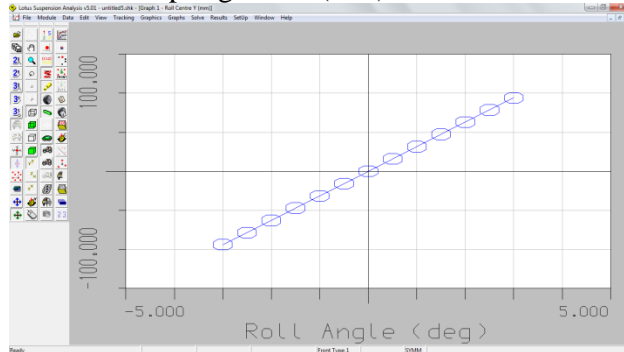


GRAPH 4: Caster angle (deg)

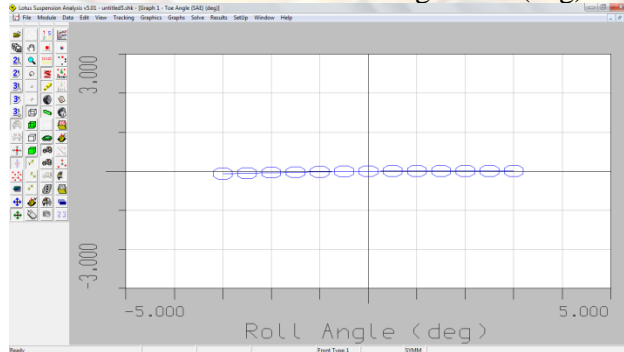


Plot of **roll graphs** for various suspension geometries

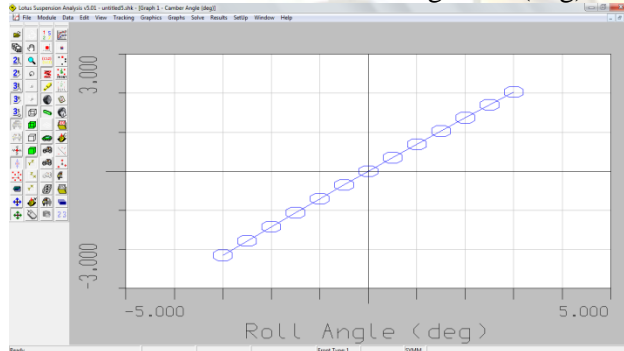
GRAPH 1: Spring travel (mm)



GRAPH 2: Toe angle (deg)



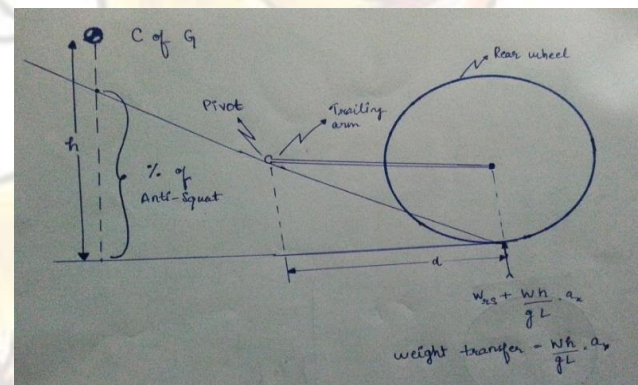
GRAPH 3: Camber angle (deg)



a) Anti-squat:-

As we know that suspension is equivalent to a trailing arm, the anti-squat performance can be quantified by analyzing the free body diagram of a rear-drive axle as shown. In figure, point "A" is the pivot of trailing arm on the body. Since the arm is rigidly fastened to the wheel hub, it has ability to transmit vertical force to the sprung mass which can be designed to counteract squat.

Diagram:-



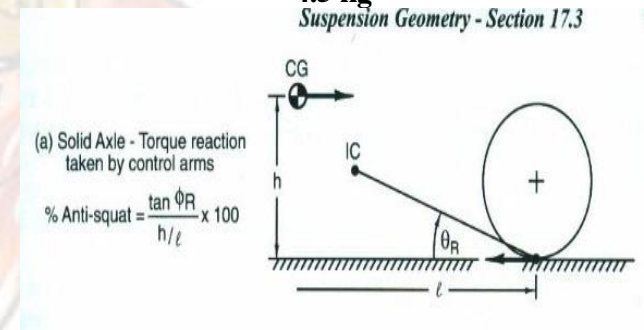
Calculations for anti-squat:-

$$\text{Weight transfer in Squat} = \frac{W \cdot h \cdot a_x}{g \cdot L}$$

$$= \frac{180 \times 228 \times 2}{9.8 \times 1828}$$

$$= 4.5 \text{ kg}$$

Suspension Geometry - Section 17.3



$$\% \text{ Anti-squat} = \frac{\tan \theta_R \times 100}{h/l}$$

$$= \frac{\tan 7.2 \times 100}{228/1375}$$

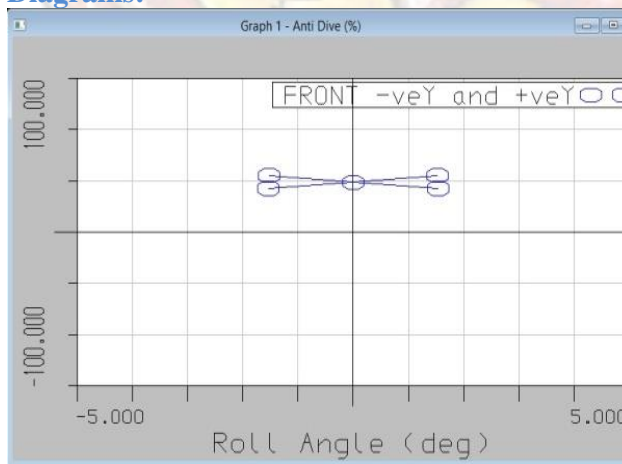
Anti-Squat and Anti-Dive Suspension Geometry

$$= 76.1\%$$

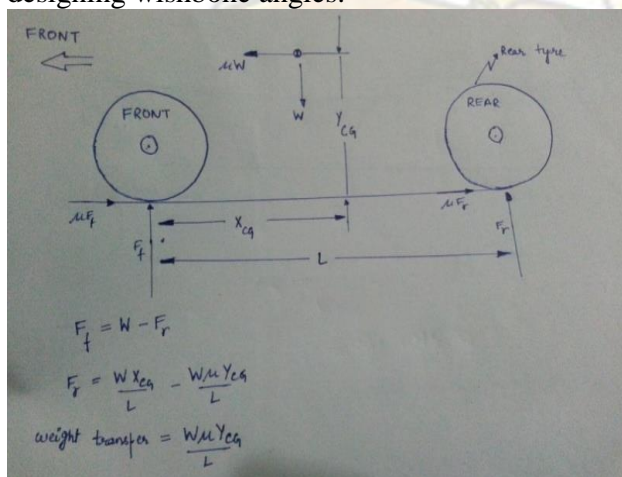
b) Anti dive:-

Anti-Dive describes the amount the front of the vehicle Dives under braking. As the brakes are applied, weight is transferred to the front and that forces the front to dive. Anti-Dive is dependent on the vehicles center of gravity, the percentage of braking force developed at the front tires vs. the rear, and the design of the front suspension.

Diagrams:-



According to the graph percentage of Anti-dive comes out to be **48%**. Normally 50% of Anti-dive is considered to be best for designing wishbone angles.



$$\text{Weight transfer in Dive} = \frac{W \times \mu \times Y_{CG}}{L}$$

$$= \frac{180 \times 0.7 \times 228}{1828}$$

$$= 15.7 \text{ kg}$$

ADVANTAGES AND DISADVANTAGES

Pros

- Double wishbone suspension provides the engineer more free parameters than some other types do.
- It is fairly easy to work out the effect of moving each joint, so the kinematics of the suspension can be tuned easily and wheel motion can be optimized.
- They also provide increasing negative camber gain all the way to full jounce travel, unlike the Macpherson strut, which provides negative camber gain only at the beginning of jounce travel and then reverses into positive camber gain at high jounce amounts.
- The double wishbone setup include easy control of the roll centers by choice of the geometry of the control arms.
- Larger suspension deflections, and greater roll stiffness for a given suspension vertical rate.

Cons

- Conversely, it may take more space and is slightly more complex than other systems like a Macpherson strut.
- Due to the increased number of components within the suspension set up it takes much longer to service and is heavier than an equivalent Macpherson design.
- At the other end of the scale, it offers less design choice than the more costly and complex multi-link suspension system.

STEERING SYSTEM:

ABSTRACT:

The Steering system has been chosen by considering the need of racing track and swift turning of our vehicle.

INTRODUCTION:

Like most things in a car, the concept of steering is simple - you turn the steering wheel, the front wheels turn accordingly, and the car changes direction. The steering of our vehicle is arranged so that the front wheels will roll truly without any lateral slip. The front wheels are supported on front axle so that they can swing to the left or right for steering. This movement is produced by gearing and linkage between the steering wheel in front of the driver & the steering knuckle or wheel.

SELECTION OF STEERING SYSTEM:

The various steering systems in consideration are: Rack and Pinion steering, Recirculating Steering and Mechanical linkage system.

To select the steering system for our vehicle, the steering department studied the applications, advantages and disadvantages of various steering system. On the basis of this study, the matrix is constructed to select the steering system as per requirement:

ADVANTAGES OF RACK AND PINION OF OVER OTHER STEERING SYSTEM:-

- It is easy to operate.
- The Contact between steering rack and pinion is free of play.
- It is compact i.e. require less space
- The idler arm (including bearing) and the intermediate rod are no longer needed.
- It is economical and uncomplicated to manufacture.
- It is easy to limit steering rack travel and therefore the steering angle.
- In this, we can change the steering ratio according to our desire like 12:1, 7:1, 10:1 etc

Type of Steering system	Weight	Ease of Operation	Cost	Free Play	Manufacturability	Total
Mechanical linkage system	4	2	3	2	4	15
Rack and Pinion steering	4	4	5	5	4	20
Recirculating Steering	2	4	2	4	2	14

Scale Used: 1-5; 5 being best

After deciding the type of Steering System, we surveyed the market for vehicles having Rack and Pinion Steering System to select

the best suited configuration to our vehicle. The list of Certain Vehicles with their steering configurations is as follows:

Vehicle	Turning Radius (feet)	Steering Ratio
Maruti 800	14.44	17:1
Tata Indigo	13.12	11:1
Maruti Zen	16.07	16:1

After doing the market survey, we decided to use steering ratio of 11:1, as it is best suited to our vehicle and race track requirements. Further it will reduce the effort required for manoeuvring.

CALCULATIONS OF TURNING RADIUS:-

The turning radius of a vehicle is given by:

$$R = \sqrt{a^2 + l^2 (\cot \delta)^2}$$

Where

a = Distance of center of gravity from rear

axle = $\frac{2l}{3}$ (For Trikes)

l = Wheel base

$$\cot \delta = \frac{1}{2} (\cot \delta_o + \cot \delta_i)$$

$$\text{Also, } \cot \delta_o - \cot \delta_i = \frac{w}{l}$$

Where, w = Track width l = Wheel Base

Assume, Inner Steering Angle, $\delta_i = 40^\circ$

Track Width, w = 4.04 ft.

Wheel Base, l = 5.5 ft.

We know that,

$$\frac{w}{l} = \cot \delta_o - \cot \delta_i$$

(Putting the values of the given in the equation)

$$\frac{4.04}{5.5} = \cot \delta_o - \cot 40^\circ$$

$$0.734 + \cot 40^\circ = \cot \delta_o$$

$$\delta_o = \cot^{-1}(1.926)$$

$$\delta_o = 27.44^\circ$$

Which is outer steering angle.

$$\text{Now, } R = \sqrt{a^2 + l^2 (\cot \delta)^2}$$

Putting the values

$$a = 3.67 \text{ ft.}$$

$$\cot \delta = 1.559$$

We get

$$R = \sqrt{\{(3.67)^2 + 5.5^2 (1.559)^2\}}$$

$$R = 9.33 \text{ ft.}$$

CALCULATIONS FOR LOCK-TO-LOCK STEERING:-

Steering ratio = 11:1

Maximum deflection of Front Wheels = 40°

Angle Turned by Steering Wheel = $40^\circ \times 11 = 440^\circ$, which is only to one side.

The entire steering goes from -40° to $+40^\circ$ giving a lock-to-lock angle at the steering wheel of 880° , or 2.4 turns ($880^\circ / 360$).

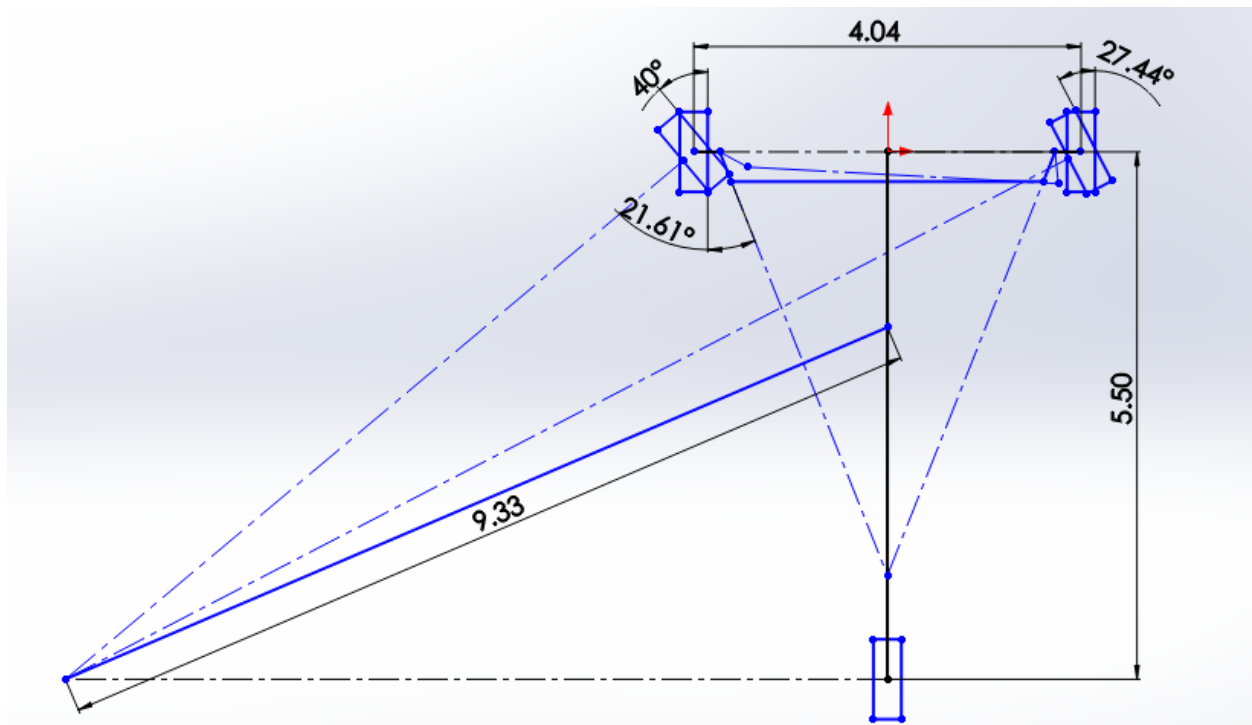


Figure: Steering Geometry Drawing

Steering Type	Rack & Pinion
Steering Ratio	11:1
Max Steering Angle	40°
Minimum Turning Radius	9.33 feet
Steering Column Height	1.03 feet
Steering Column Length	2.57 feet
Length Of Rack	0.894 feet
Length Of Tie Rod	1.215 feet
Steering Arm Length	0.33 feet
Ackerman Angle	21.614°

Table: Steering Geometry Summary

TRANSMISSION:

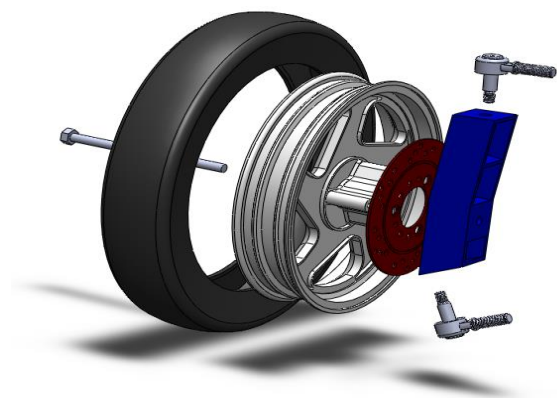
INTRODUCTION:

A lot of emphasis has been placed on the design of power train. In design of the drive train the optimization of several desired characteristics are being kept in mind including acceleration, top speed, and durability. Here we are using a D.C brushless Motor with capacity of 48V-10A which is capable of providing us a torque of max 4 N-m, thus our main objective is to harness the power available efficiently to deliver it to the tires for peak performance. We are using chain drive for transmission of power from motor to the wheel with a constant gear ratio of 2.9:1. We are going to mount this drive directly on the wheel, thus reducing the loses. The motor here we are using is D.C Brushless having power of 0.69 hp and has the capacity to produce maximum torque of 4 Nm and maximum rpm of 3500. The gear ratio here we are using is 2.93:1. The dimension of tire we are using for best output is 18 inches.

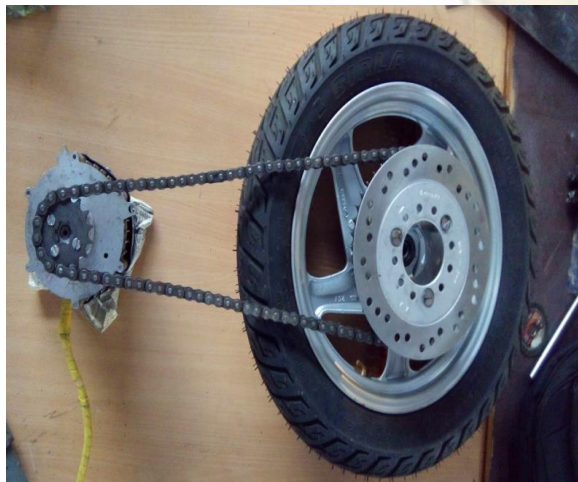
The design of wheel assembly has the following component as shown:-

PARAMETERS

MOTOR	D.C MOTOR (48V-10A)
TYPE	BRUSHLESS MOTOR
MOTOR POWER	0.69 hp
MAX TORQUE	10 N-m
MAX. RPM	3500
TRANSMISSION	Chain Drive
Gear Ratio	2.93:1
Tire	18*12*3.5
Max. Speed	45 kmph
Max. Traction	51.8 N
Max. Torque	11.72 N-m



Initially we were using A.R CVT for transmitting power from motor to the wheel but due to change of motor with specification (12V-60A) to (48V-10A), the controlling unit also changed so we are getting the required RPM and to reduce the losses we decided to use simple transmission of Chain Drive with a constant Gear Ratio of 2.93 for good traction.

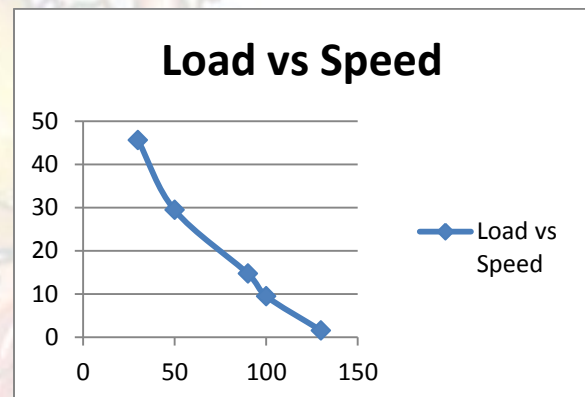


CALCULATIONS:-

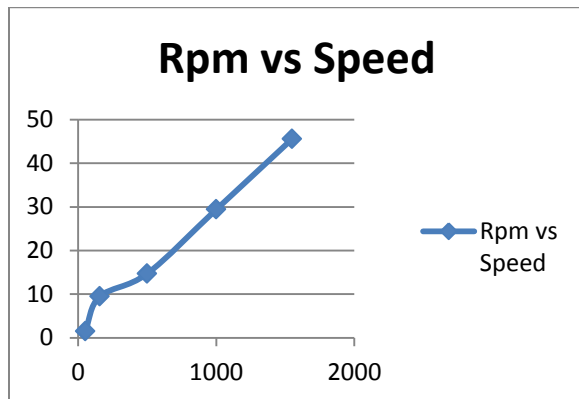
All the calculations are performed on the specification of the motor i.e. the torque and power we are obtaining from the motor. The basic calculations are as follows:

RPM	LOAD	TORQUE	SPEED	Gear Ratio
1550	30	0.825	45.56708	2.93
1000	50	1.375	29.39812	2.93
500	90	2.475	14.69906	2.93
156	100	2.75	4.586106	2.93
52	130	3.575	1.528702	2.93
150	130	3.575	4.409717	2.93
100	140	3.85	2.939812	2.93

The graph between load and speed is shown below:



The Graph between Rpm and speed is given as:



FORMULA USED FOR CALCULATION:

1. **POWER OUTPUT** = $\frac{2\pi NT}{60}$
2. **TRACTION IN THE WHEEL** = Force – Rolling Resistance
3. **FORCE** = Mass \times acceleration
4. **SPEED OF WHEEL** = $\frac{\pi ND}{60}$
5. **FINAL TORQUE** = Gear Ratio \times Initial torque
6. **FINAL RPM** = $\frac{\text{Initial rpm}}{\text{gear ratio}}$
7. **TORQUE** = Force \times perpendicular distance
Where
N = Speed in RPM
T = Torque
D = Diameter of the wheel

INNOVATION

INTRODUCTION:

Innovation is a most important part of our vehicle. The motto of innovation is safe the driver and vehicle from damage or accident.

MOTTO:-

- Protect the driver from accident.
- Protect vehicle from the damage.
- Make driver comfortable.
- Protect battery to explode due to overcharge.

LIST OF INNOVATIONS:-

1. Ultrasonic sensor
2. Temperature indicator
3. Battery charge indicator
4. Seat belt sensor

1. ULTRASONIC SENSOR:

Ultrasonic work on a principle similar to radar or sonar which evaluates attributes of a target by interpreting the echoes from radio or sound waves respectively. Ultrasonic sensors generate high frequency sound waves and evaluate the echo which is received back by the sensor. Sensors calculate the time interval between sending the signal and receiving the echo to determine the distance to an object.

Functions:

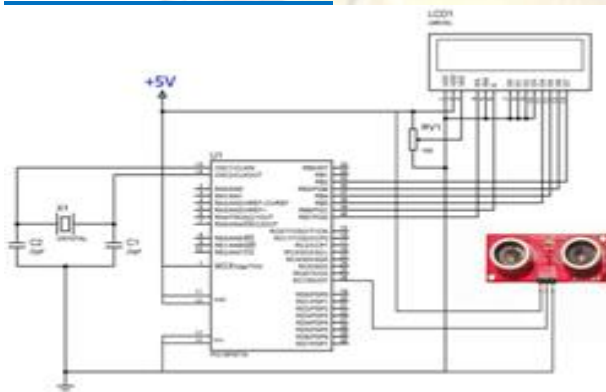
- To measure optical distance from the vehicle.
- Help in parking the vehicle.
- Save vehicle from the accident or damage.

Component:-

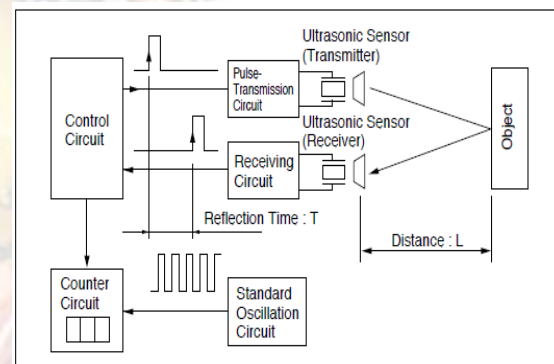
SPECIFICATION	QUANTITY
Ultrasonic receiver	1
Ultrasonic transmitter	1
LMO16L	1
PCB board	2
PIC16F877A	1
Capacitor(22pf)	2

tutorial we will learn to interface an Ultrasonic Distance Sensor with PIC Microcontroller.

Here for demonstration we are using Rhydolabz Ultrasonic Distance Sensor with ASCII Output. It can be easily interfaced with a PIC Microcontroller using USART by just connecting the output pin of the sensor to RX pin of the microcontroller. In every 500ms this sensor transmits an ultrasonic burst and listens for its echo. The sensor sends out ASCII value corresponds to the time required for the ultrasonic burst to return to the sensor. The UART of the sensor is operates at a baud rate 9600 and the sensor can be powered by a 5V DC Supply. The ASCII output of the sensor will be equal to the distance to the obstacle in centimeter (cm). The sensor has three pins...

CIRCUIT DIAGRAM:-**WORKING:-**

Ultrasonic Distance Sensors are the best sensor which provides stable, accurate, precise, non-contact distance measurements from 2cm to 4m. Ultrasonic Sensors can be used to measure distance between moving or stationary objects. Being very accurate and stable, these devices find large number of applications in robotics fields. For example it can be used as an excellent replacement for IR sensors in a Micro mouse. In this



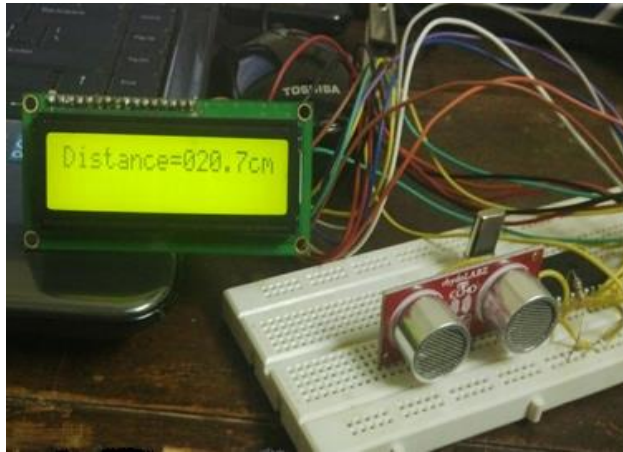
Principles of Measuring Distance

Vcc - +5V DC Supply to the Sensor

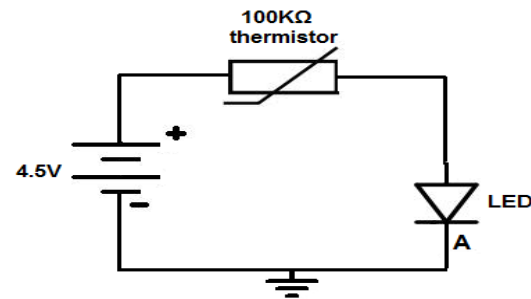
GND – Ground Level of the Power Supply

SIG – Signal, Serial Data Out

Ultrasonic Distance Sensor interfaced with PIC Microcontroller:



CIRCUIT DIAGRAM:-



WORKING:-

At room temperature, the thermistor will offer very high resistance, near its rated value of $100K\Omega$. At this resistance, practically no current flows so the LED does not get triggered.

However, when the thermistor is exposed to a significant amount of heat, its resistance will drop significantly. Enough current now flows through the circuit to trigger the LED. And this is how this heat alarm circuit works.

2. TEMPRATURE INDICATOR:

To indicate the overheating of the battery we used temperature indicator for the safety proposes of the driver. Some time due to overcharging heat will produce by battery and possibility of explored will be increased. Due to this possibility temperature indicator will be used.

Requirement:-

- To indicate over heating of battery.
- To safe driver from explore of battery.

Component:-

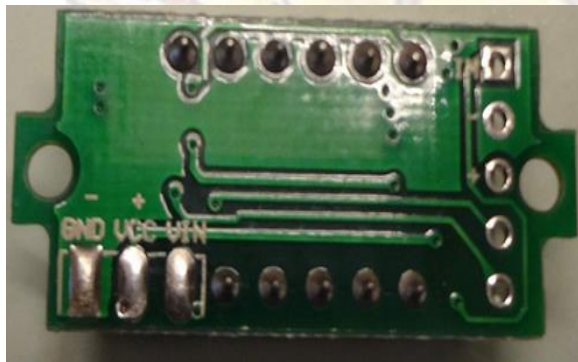
COMPONENT	QUANTITY
THERMISTOR	140W
SUPPLY	19V
LED	7.2A

3. BATTERY INDICATOR:

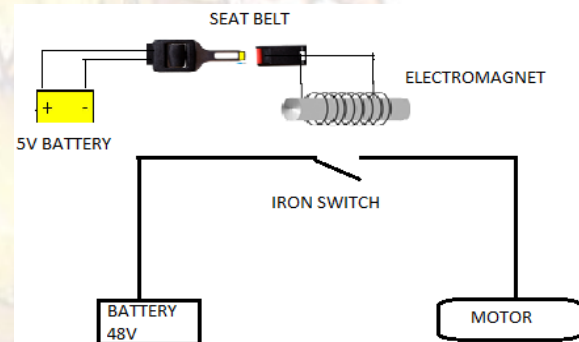
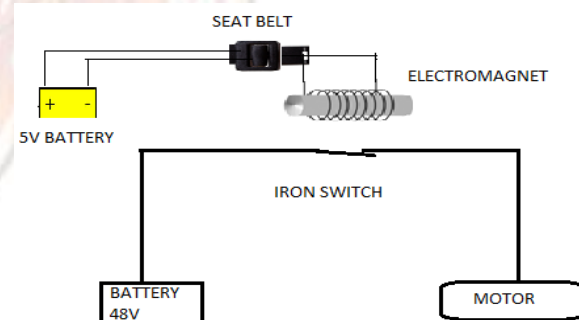
A Battery indicator is a device which gives information about a battery. This will usually be a visual indication of the battery's state of charge. It is particularly important in the case of a battery electric vehicle.

Requirement:-

- To indicate the battery charge level.
- To show low battery.
- Auto cut the connection at over charging.

DIAGRAM:-**COMPONENTS:-**

COMPONENT	QUANTITY
SEAT BELT	1
Electromagnetic coil	1
5V SUPPLY	1
IRON SWITCH	1
IRON CORE	1

CONNECTION:-*When seat belt is open**When seat belt is closed***4. SEAT BELT SENSOR:**

To protect the driver seat belt is a most important part in vehicle. We used a circuit in which when a seat belt end is connected each other than the car will be start.

Requirement:-

- To protect the driver from shock.
- Immediately cut the connection of motor to open the belt.
- Motor is only start if the belt will be closed, so driver is safe.

WORKING:-

At first when a seat belt is open then no EMF will be produced so iron switch will be open, the circuit shown in first fig. When belt is closed then the electromagnetic circuit is completed and EMF will be produced by the electromagnetic coil and iron switch is closed for EMF effect. Connection is completed and motor will be in running condition.

